

Probability-based assessment of the durability characteristics of concretes manufactured using CEM II and GGBS binders

Dr Ciaran McNally¹ & Dr Emma Sheils

Abstract

This paper presents an overview of an investigation into the durability characteristics of blends of GGBS with CEM II/A Portland cements. The introduction of the Emission Trading Scheme has focussed attention on the carbon footprint arising from concrete construction, leading to many countries employing cementitious binder combinations not previously used. In Ireland for example concrete practice has recently changed to allow the addition of GGBS to CEM II/A cements at the concrete mixer, dependent on these blends providing adequate durability. To demonstrate this performance, specific research was conducted into the influence of GGBS addition on resistance to chloride ingress and carbonation, as well as compressive strength. The data from the testing was then used as input parameters for a number of probabilistic models describing chloride and carbonation related deterioration mechanisms. The influence of GGBS content on the expected service life is determined and compared to other research in this area.

Keywords: Concrete Technology; Deterioration; Durability; Performance Based Design; Prediction Models; Risk & Probability Analysis

1. Introduction

Significant national funds are being invested worldwide in the construction of infrastructure required to support society's needs. The high cost of constructing this infrastructure means that it is important that durable concrete is used in this process. Failure to provide concrete with adequate durability will inevitably result in undesired early repairs where harsh service environments are often encountered. The cost implications associated with this are severe. For example, in the US it is estimated that \$25 billion is spent each year on the repair of wastewater infrastructure [1]; the report Bridging the Gap [2] addressed the state of the US national bridge stock and found that 25% of the 590,000 bridges in the US can be described as 'deficient' or 'functionally obsolete'. The budgets involved will change from country to country but the scale of the problem is clear.

¹ Dr. Ciaran McNally UCD School of Civil, Structural & Environmental Engineering, University College Dublin, Newstead, Belfield, Dublin 4, IRELAND.
e-mail: ciaran.mcnally@ucd.ie

In this light it is clear that more durable concrete structures are required, and towards this end secondary cementitious materials (SCM) are increasingly being used in concretes where durability is a concern. Improved durability has been achieved by the addition of ground granulated blast furnace slag (GGBS) [3, 4], fly ash [5, 6], silica fume [7] and metakaolin [8]. It is noteworthy that much of the research cited above into the improved durability performance of concretes incorporating SCM was conducted using CEM I type Portland cements. In Europe these cements are primarily manufactured using 95% clinker, with 5% minor additions. The construction industry however is quite dynamic, and in response to environmental pressures significant changes have been made in the range of Portland cements that are now commercially available. The production of cement clinker is an energy intensive process and the manufacture of 1 tonne of clinker leads to the emission of approximately 0.95 tonnes of CO₂ [9]. In an effort to reduce this, and in response to the Emissions Trading Scheme under the terms of the Kyoto Protocol, significant changes were required. In this context it is not surprising that cement manufacturers are increasingly moving away from the production of CEM I Portland cements and towards more sustainable and less carbon intensive construction practices. This has been observed in countries such as Ireland and the United Kingdom where CEM I is no longer the dominant cement available and has been replaced with less CO₂ intensive CEM II products.

The current European standard for cement production EN 197 [10] allows for the use of up to 27 different cements in concrete production. These range from CEM I which uses 95-100% clinker to CEM III/C which can utilise as little as 5-19% clinker. An extract from EN 197 is shown in Table 1 which lists the most common of these cements. The use of these cement types varies considerably across Europe and until recently the production was largely decided by the availability of key ingredients such as limestone, blast-furnace slag, siliceous fly ash etc. However the introduction of the Emissions Trading Scheme as described above has significantly adjusted the dynamics of the industry as there are now potentially costly financial penalties associated with using significant amounts of clinker. National markets that had previously been dominated by CEM I were now having to adapt to the implications of working with alternate cement types such as a CEM II/A-L and CEM II/A-V. While the satisfactory performance of the new cement types is well established, the durability characteristics of concretes manufactured using these cements in combination with SCM such as GGBS is less well understood and the motivation behind this paper. In particular this paper will focus on the mixer addition of GGBS to the concrete; this practice is commonly used in countries that do not have an indigenous steel industry, resulting in GGBS being less freely available. In such countries granulated blast furnace slag is often imported by GGBS manufacturers.

2. Testing methodologies

To determine the durability of combinations of CEM II/A Portland cements with relatively high quantities of GGBS, a series of performance tests were selected. A number of key concrete durability aspects were considered for inclusion in this study: resistance to chloride ingress, resistance to carbonation and strength development. Resistance to sulfate attack is not easily measured using concrete samples and as such is not included in this paper. Freeze-thaw testing was also not included as appropriate service life models are not yet sufficiently developed. Based on these concrete durability criteria, a series of tests were required to determine the performance of the concrete mixes. The tests were selected to be conducted in a reasonable time frame to allow direct comparison of the performance of the various concrete mixes.

For these tests, a series of concrete mixes were designed to reflect the mix designs featured in the Irish National Annex to EN206. These comprised binder contents of 320 and 400 kg/m³ and water/binder ratios of 0.55 and 0.45 respectively. The basic mix designs are listed in Table 2. The cementitious binders used in the testing programme were a combination of the following:

- CEM II/A-L: class 42.5 Portland limestone cement
- CEM II/A-V: class 42.5 Portland fly-ash cement
- CEM III/B: class 32.5 Blastfurnace cement
- Ground granulated blast furnace slag (GGBS)

The coarse and fine aggregates used were predominantly limestone and the maximum particle size was 20mm. Samples were taken from each of the cementitious binders and tested for chemical composition using a standard XRF technique; the results of this are presented in Table 3. A Sympatec Helos Particle Size Analyser was used to determine the particle size distribution of the binders and these are presented in Fig. 1. Inspection of the data shows that the mean particle size for the CEM II/A-L, the CEM III/B and the GGBS to be 20.4, 16.4 and 14.0 µm respectively, while the CEM II/A-V has a mean particle size of 43.3 µm. The full list of binder combinations tested is shown in Table 4.

2.1 Resistance to chloride ingress

Traditional test methods to quantify this resistance involve the long-term immersion of concrete samples within chloride-rich environments. While these experiments have been shown to produce reliable diffusion coefficients [11], they have the disadvantage of being very slow. Tang and Nilsson [12] developed an accelerated test-method whereby the chloride diffusivity of a concrete sample may be determined by the application of an electric field across a concrete sample immersed in a sodium chloride solution. The depth of chloride

penetration is visually determined by staining with silver nitrate and is used to determine a non-steady state migration coefficient. Tang and Nilsson have also shown how this can be converted to produce an effective diffusion coefficient, D_{eff} ; this is equivalent to the more familiar apparent diffusion coefficient. This easy-to-use method is more commonly known as the Rapid Chloride Migration (RCM) test and was formalised in Nordtest NT Build 492 [13].

The RCM test is typically measured on cylindrical test specimens. A series of concrete slabs were cast that were 300mm square and 100mm deep. The slabs were cured for 3 weeks in water at 20°C, after which they were moved to a constant temperature room with a relative humidity of approximately 65%. It is worth noting that the RCM test does not specify a curing environment for concrete samples; this curing environment was selected as it matches that described in durability tests such as EN 12390 Part 10 on carbonation resistance. When the samples were 90days old, 100mm cores were taken from this slab; the cores were then cut 25mm from each end to produce a test sample that was 100mm in diameter and 50mm thick. This was then subjected to the preconditioning and testing environments as specified in NT Build 492. Tests are conducted on 2 samples and the mean diffusion coefficient calculated. If both test results were within 10% of the mean then the result was accepted; if not, then an additional test was conducted to confirm the chloride resistance.

2.2 Resistance to carbonation

Resistance to the diffusion of CO₂ into the concrete matrix was determined using an accelerated carbonation testing unit that was designed and built in-house. The test chamber allows the user to set the desired temperature and CO₂ content. Relative humidity is not controlled but experience has shown that the system is constant in this respect at approximately 60±4%. The carbonation chamber is instrumented with sensors to measure CO₂ content, temperature and relative humidity. A LabView programme was written to control the test environment and is connected to a CO₂ supply and an internal heater. A circulation fan is also fitted inside the chamber to ensure a consistent test environment and typical target test conditions are a CO₂ content of 5% and a temperature of 20°C.

The tests were conducted on 100mm cube samples stored in the test chamber for preset time periods. The cubes were cured for 3 weeks in water at 20°C, after which they were moved to a constant temperature room with a relative humidity of approximately 65% for a further 7 days before testing. Samples were removed from the chamber after 7, 28 and 56 days and split in indirect tension. These were then treated using a phenolphthalein indicator and the carbonation depth measured by callipers on a set of 3 samples.

2.3 Compressive strength

The compressive strength of the various mixes was determined using the standard method of casting 100mm concrete cubes and crushing them at preset time intervals up to 90 days.

3. Results

3.1 Chloride ingress

The RCM test was conducted on concrete samples after 90 days to produce a non-steady state migration coefficient. The data was then further processed following the procedures developed by Tang & Nilsson [12] to produce an effective diffusion coefficient. Average values were calculated and these are presented in Table 5. It can be seen that the highest diffusion coefficients all correspond to the binder combinations that contained 100% CEM II/A binder. The CEM II/A-L performed slightly worse than the CEM II/A-V and this is observed for both sets of samples (i.e. 320 and 400 kg/m³ of binder). In all cases the addition of 50% and 70% GGBS lead to significant reduction in the effective diffusion coefficient. There is no indication as to which GGBS replacement level resulted in optimal chloride resistance – it was observed that the addition of 50% or 70% GGBS produced binder combinations that were approximately equivalent. From an industry perspective, it is also worth noting that the factory produced CEM III/B contains approximately the same amounts of GGBS and clinker as a mix produced using a CEM II/A with a 70% GGBS replacement level. It can be seen that the effective diffusion coefficients for mixes A3, A6 and A7 are approximately equivalent, with D_{eff} values ranging from $0.77-1.73 \times 10^{-12} \text{ m}^2/\text{s}$. Similar behaviour is observed between samples B3, B6 and B7, with D_{eff} values ranging from $0.81-1.07 \times 10^{-12} \text{ m}^2/\text{s}$ suggesting that addition of GGBS at the mixer leads to equivalent concrete performance. These results compare well with that recorded by Yeau and Kim [14] who found that increased addition of GGBS results in continued improvement in resistance to chloride penetration. This testing however only made use of CEM I cements.

While the results presented above are of interest in comparing cementitious binders, they do not allow for the time dependent nature of the hydration reaction. This is discussed in more detail in the later section on service life prediction.

3.2 Carbonation

The average carbonation depth was also determined using the procedure described above after 7, 28 and 56 days at elevated CO₂ levels. The results for 7, 28 and 56 days exposure are also presented in Table 5. It can be seen that in all cases, the addition of GGBS has resulted in increased depths of carbonation. This is in agreement with the findings of Papadakis [15] who found that SCM when used as a cement replacement, lead to increased carbonation depths. The chemistry behind this is also discussed by Glass *et al.*

[16] who studied the influence of SCMs on the acid neutralisation capacity of cementitious binders. It was found that the pore solutions of GGBS binders possessed significantly less resistance to pH reduction than OPC binders. This was attributed to a reduced calcium hydroxide produced during hydration and is in agreement with the results produced in this research. Al-Otaibi [17] also investigated the influence of a 60% GGBS replacement level on the durability characteristics of concrete manufactured using CEM I and found that this resulted in improved chloride resistance but decreased carbonation resistance.

3.3 Compressive strength

The compressive strength of the various binder combinations was determined and these are presented in Figures 2 and 3. It can be seen that for each binder content the highest strengths were associated with the CEM II/A-L cement. The use of a 50% GGBS replacement level resulted in almost unchanged strength levels. Similar trends are reported by Sengul and Tasdemir [18] who again worked with CEM I cements. The addition of 70% GGBS however resulted in a significant decrease in compressive strength, with reduction of between 17 - 24% for the CEM II/A-L and 24 – 36% for the CEM II/A-V. This is not in agreement with trends observed for CEM I cements where researchers such as Barnett *et al.* [19] found that the addition of up to 70% GGBS resulted in little change to the 28 day compressive strength. This however may be explained by the reduced activity of CEM II cements relative to CEM I cements which would influence the hydration of binder combinations featuring high quantities of GGBS.

4. Probabilistic service life prediction

While the above data allows comparison between the various binder combinations, it does not offer sufficient insight with respect to the service life that may be expected from these concretes. When designing structures, the whole life performance of the structure including possible future maintenance and repair actions must be considered. As well as direct implications of maintenance and repairs, thought should also be given to indirect costs such as user delay costs which can be significant (e.g. due to traffic delays, lane closures etc). To provide this information probabilistic modelling has been carried out using the experimental results described above. These models will determine the service life implications of using the selected binder combinations and allow comparison of the relative performance of the mixes over time.

4.1 Structural application

A scenario is offered of a reinforced concrete bridge in service subjected to chloride related deterioration and carbonation related deterioration. Commonly used service life models are

employed for each form of deterioration, and no interaction is assumed between the two mechanisms. Mean material parameters are based on the test data presented in this paper. Distributions are assigned to each random variable and a Monte Carlo simulation approach is employed. The probability of corrosion initiation due to chloride ingress and carbonation is generated for each of the 14 concrete mixes tested.

4.2 Parameters for chloride induced corrosion

For the case of chloride induced corrosion, an equation derived from Fick's second law of diffusion is commonly used to predict the chloride concentration at a certain depth after a certain period of time. Pack *et al.* [20] recently utilised this equation, allowing for the time dependent nature of the diffusion coefficient. The chloride concentration at a given depth (e.g. cover depth) depends on the time, the rate of chloride ingress and the surface chloride concentration. Assuming an initial chloride concentration of zero, it is possible to determine the chloride concentration at the cover depth, X , for a service life of $t = 50$ years and $t = 100$ years using equation (1) below [21, 22]:

$$C(X,t) = C_{sn} \left[1 - \operatorname{erf} \left(\frac{X}{2\sqrt{D_m t}} \right) \right] \quad (1)$$

where C_{sn} is the surface chloride concentration and D_m is the mean effective chloride diffusion coefficient for the exposure duration, t , calculated using equations (2) and (3).

$$D(t) = D_R \left(\frac{t_R}{t} \right)^m \quad (2)$$

$$D_m(t) = \frac{1}{t} \int_0^t D(\tau) \cdot d\tau \quad (3)$$

where D_R is the chloride diffusion coefficient at a reference time t_R (in this case 90 days, as listed in Table 5). The parameter m is an age factor used to describe the evolution of the chloride diffusion coefficient over time. Based on the work of Pack *et al.* [20], this parameter is taken as 0.06 for 100% OPC binders and 0.23 for binders containing GGBS.

Breakdown of the passive layer and corrosion of the reinforcing steel is taken to begin when the chloride concentration at the cover depth is greater than the critical chloride concentration, C_{cr} . The bridge is assumed to have a cover depth of 50mm, a typical cover depth for structures in aggressive chloride environments. The critical chloride concentration for initiation of corrosion, C_{cr} , is taken as 3.35 kg/m^3 and the constant surface chloride level, C_{sn} , is taken as 2.95 kg/m^3 . Angst *et al.* [23] recently conducted a review of critical chloride concentrations and found conflicting evidence regarding the influence of GGBS on critical chloride concentrations. Schiessl and Breit [24] suggested that GGBS will lead to an increase in critical chloride concentration, while Gouda and Halaka [25] suggested a decrease and Oh

et al. [26] suggested no change. In this context it is reasonable to assume a constant critical chloride concentration for all mixes. A probability distribution and coefficient of variation (COV) are assigned to each of the parameters, and are presented in Table 7. These values are based on previous work conducted by Val and Stewart [27] on chloride induced corrosion. By introducing the time-dependent diffusion coefficients from Table 6, it is possible to observe the effect of the GGBS replacement level on the probability of corrosion initiation at a given time and thus, an indication of the expected service life of the structure. A Matlab programme was developed to generate 1,000,000 realisations of each random variable given the specified mean, COV and distribution. These were then used with (1) to generate a distribution of chloride concentration at a cover depth of 50mm for a service life of 50years and 100years for each mix. By also generating 1,000,000 realisations from the distribution of critical chloride content, it was possible to determine the probability of corrosion initiation from the proportion of realisations where the chloride concentration was greater than the critical chloride concentration [28].

4.3 Parameters for carbonation induced corrosion

It has been well documented that the depth of carbonation in concrete is proportional to the square root of time [29]. On this basis, Papadakis *et al.* [30] developed and experimentally verified a model predicting the process of concrete carbonation. This was further developed to include an efficiency factor, taking account of the carbonation resistance properties of different SCMs. Papadakis and Tsimas [31] found that the carbonation depth can be calculated from:

$$x_c = \sqrt{\frac{2 D_{e,CO_2} (CO_2 / 100) t}{0.218(C + kP)}} \quad (4)$$

where x_c is the carbonation depth; D_{e,CO_2} is the effective CO_2 diffusivity of concrete; t is time; CO_2 is the CO_2 content of air at the concrete surface (%); C is cement content (kg/m^3); k is the efficiency factor of the SCM with respect to CO_2 diffusion and P is the SCM content (kg/m^3). Furthermore Papadakis and Tsimas [31] have shown that the CO_2 effective diffusion coefficient is heavily influenced by the relative humidity:

$$D_{e,CO_2} = 6.1 \times 10^{-6} A \left(1 - \frac{RH}{100}\right)^{2.2} \quad (5)$$

where A is a function of the cement content, the carbonation efficiency factor, the SCM content and the water content, and is a constant parameter for each mix.

Based on the test data reported in Table 5, it is possible to plot the depth of carbonation against the square root of time to determine the effective CO_2 diffusivity of the concrete, D_{e,CO_2} . Using the results for D_{e,CO_2} , the value of A in (5) is determined for each mix

using a relative humidity of 65% (as per experiment). Once the constant A is determined, the effective CO₂ diffusivity of each mix can be calculated using (5) for varying values of relative humidity. Rearranging (4), the time for carbonation to reach a selected cover depth of 50mm can then be determined.

The parameters of the random variables used in the probabilistic model for carbonation are presented in Table 7. Ambient CO₂ conditions can never fall below the atmospheric level of 0.039%; as such a lognormal distribution with a mean of 0.05% was employed to describe the variation in CO₂ concentration. Although it is recognised by the authors that global warming may increase CO₂ levels significantly in the future, having implications on the corrosion risk due to carbonation [33], for this paper current CO₂ levels are assumed. The relative humidity was modelled as a deterministic parameter and a value of 75% was taken to be representative of an outdoor environment; this excludes the influence of wetting and drying cycles and allows comparison between the cement blends under test. Using this approach it is not necessary to determine difficult material parameters such as the efficiency factor of the SCM with respect to CO₂ as this can be coupled with the effective diffusion coefficient. Again, 1,000,000 realisations of each random variable were generated. For each mix they were used with equations (4) and (5) to generate a distribution of the time for carbonation to reach the cover depth. From this distribution, the probability of carbonation reaching the cover depth was determined for each over the service life of the structure.

4.4 Model uncertainties

The approaches described above do not include model uncertainties as a component of the prediction model. This is justified by the focus of the paper, which is intended to highlight the relative difference between the expected service life of concretes manufactured from various binder combinations with respect to carbonation induced corrosion and chloride induced corrosion. The addition of model uncertainties would have the effect of increasing the uncertainty associated with the overall results presented in Figures 4-6. Since the model uncertainty is associated with the prediction model rather than the deterioration parameters, this would not impact on the overall conclusions of the paper. This approach has also been used by other authors addressing reliability based approaches [34, 35, 36, 37, 38, 39].

4.5 Results of service life prediction

Sample results of the probabilistic modelling for chloride induced corrosion after 50years and 100 years are shown in Figures 4 and 5 respectively where the probability distribution function (pdf) for chloride concentration at the cover depth is illustrated along with the pdf for critical chloride content. To illustrate the variation between mixes, the pdf for two different binder combinations (A1 and A5) is presented in both figures. The overlap of the chloride

concentration and critical chloride concentration distributions is indicative of the probability of corrosion initiation due to chloride ingress. Fig. 4 illustrates that there is a higher probability of corrosion initiation for mix A1 compared with mix A5. Fig. 5 demonstrates how the probability of corrosion initiation increases over time for both mixes. From the analysis it is possible to determine the cumulative probability of corrosion initiation due to chloride ingress at selected times in the structures service life. For this particular case service lives of 50 and 100 years are chosen and the results are presented in Table 8. From the table, it can be seen that the concrete mixes containing 100% Portland cement binders (e.g. A1, A4, B1, and B4) are more likely to undergo chloride induced corrosion at an early stage in their service life.

The results of the probabilistic modelling for carbonation induced corrosion are shown in Fig. 6. From the figure it can be seen that the binders containing high GGBS contents (e.g. A6, B6, A3, A7, and B3) are much more likely to suffer from carbonation related corrosion, albeit at a relatively long time after construction. Using the data in Fig. 6 it is possible to produce cumulative distribution curves and determine the probability of carbonation induced corrosion initiation at service lives of 50 and 100 years. The results are also presented in Table 8.

5. Concluding remarks

The results of the probabilistic service life prediction show that the addition of GGBS plays a significant role in achieving the targeted service life. The cementitious binders that do not contain any GGBS display a probability of chloride induced corrosion after 50 years of almost 0.25, indicating that there would be higher maintenance and repair costs for structures constructed using this type of concrete, if exposed to aggressive marine or salt spray environments. The substitution of 50% to 70% GGBS for CEM II/A significantly reduces the chloride diffusion coefficient and this is reflected in the low probability of corrosion after 50 years. For example, comparing mixes A1 and A3, the effect of using CEM II/A-L with 70% GGBS replacement rather than just CEM II/A-L is to reduce the probability of chloride induced corrosion after 100 years from 0.28 to 0.02; this would have very significant implications on the maintenance and repair requirements over the lifetime of the structure. It is also interesting to note that the expected service life associated with using a CEM III/B cement is in all cases quite similar to that observed with a CEM II/A-L with 70% GGBS replacement. This suggests that addition of GGBS at the concrete mixer produces a binder of equivalent performance to a binder where GGBS is added in a factory setting.

For the case of carbonation induced corrosion it can be observed that the poorest performance is associated with the highest GGBS replacement level, again in agreement with the work of Papadakis [15]. The concrete produced using GGBS has a more dense

microstructure, but also has significantly less carbonatable material. It is noteworthy however that this still results in very low probabilities of corrosion after 50 years, and acceptably low values after 100 years; as such, it is unlikely to influence the repair and maintenance requirements (or costs) over the service life of the structure. This slow time-frame associated with carbonation induced corrosion may also be used to justify the use of uncoupled chloride/carbonation deterioration models. The pace of the chloride and carbonation ingress mechanisms differ drastically, meaning that any interaction between the two is unlikely.

Finally, it is notable that in almost all cases the GGBS has performed better when combined with the CEM II/A-L than with the CEM II/A-V; this effect is magnified at the higher GGBS replacement levels. The chemical composition of the CEM II/A-L and the CEM II/A-V is given in Table 3 and shows the various oxides to be present as expected. It is instead postulated that the reason for this different performance is due to the grinding process and the particle size of the final cementitious product, shown in Fig. 1. This increased particle size will lead to a reduction in the activity of the CEM II/A-V and this will impact on energy available to promote the GGBS hydration reactions. This is reflected in reduced compressive strengths and poorer durability characteristics. It should be noted that the CEM II/A-V still meets the technical cement production requirements. This highlights the benefits that can be achieved by using significant quantities of GGBS, but also the sensitivity of the GGBS hydration reactions at high replacement levels.

References

- [1] Congressional Budget Office, 2002. *Future investment in drinking and wastewater infrastructure*. ISBN 0160512433. Washington: Congressional Budget Office.
- [2] American Association of State Highway and Transportation Officials (AASHTO), 2008. *Bridging the gap: Restoring and rebuilding the nations bridges*. ISBN 9781560514251. Washington: AASHTO.
- [3] Luo, R., Cai, Y., Wang, C. and Huang, X., 2003. Study of chloride binding and diffusion in ggbs concrete. *Cement and Concrete Research*, 33 (1), 1-7.
- [4] Hester, D., McNally, C. and Richardson, M.G., 2005. Study of the influence of slag alkali level on the alkali-silica reactivity of slag concrete. *Construction and Building Materials*, 19 (9), 661-665.
- [5] Bijen, J., 1996. Benefits of slag and fly ash. *Construction and Building Materials*, 10 (5), 309-314.
- [6] Chindaprasirt, P., Chotithanorm, C., Cao, H.T. and Sirivivatnanon, V., 2007. Influence of fly ash fineness on the chloride penetration of concrete. *Construction and Building Materials*, 21 (1), 356-361.
- [7] Song, H.W., Jang, J.C., Saraswathy, V. and Byun, K.J., 2007. An estimation of the

- diffusivity of silica fume concrete. *Building and Environment*, 42 (3), 1358-1367.
- [8] Gruber, K.A., Ramlochan, T., Boddy, A., Hooton, R.D. and Thomas, M.D.A., 2001. Increasing concrete durability with high-reactivity metakaolin. *Cement and Concrete Composites*, 23 (6), 479-484.
- [9] Van Oss, H.G. and Padovani, A.C., 2003. Cement manufacture and the environment: part II. Environmental challenges and opportunities. *Journal of Industrial Ecology*, 7 (1), 93-126.
- [10] British Standards Institution, 2000. BS EN 197-1: *Cement - Part 1: Composition, specifications and conformity criteria for common cements*.
- [11] McNally, C., Richardson, M.G., Evans, C. and Callanan, T., 2005. Determination of chloride diffusion coefficients for use with performance-based specifications. In: Dhir, R.K., Harrison T.A. and Newlands, M.D. eds. *Proceedings of the 6th international congress on global construction*, Dundee, Scotland, 321-327.
- [12] Tang, L. and Nilsson, L.O., 1993. Rapid determination of the chloride diffusivity in concrete by applying an electric field. *ACI Materials Journal*, 89 (1), 49-53.
- [13] Nordtest, 1999. *NT Build 492: Chloride migration coefficient from non-steady-state migration experiments*.
- [14] Yeau, Y.Y. and Kim, E.K., 2005. An experimental study on corrosion resistance of concrete with ground granulate blast-furnace slag. *Cement and Concrete Research*, 35 (7), 1391-1399.
- [15] Papadakis, V.G., 2000. Effect of supplementary cementing materials on concrete resistance against carbonation and chloride ingress. *Cement and Concrete Research*, 30 (2), 291-299.
- [16] Glass, G.K., Reddy, B. and Buenfeld, N., 2000. Corrosion inhibition in concrete arising from its acid neutralisation capacity. *Corrosion Science*, 42 (9), 1587-1598.
- [17] Al-Otaibi, S., 2008. Durability of concrete incorporating GGBS activated by water-glass. *Construction and Building Materials*, 22 (10), 2059-2067.
- [18] Sengul, O. and Tasdemir, M.A., 2009. Compressive strength and rapid chloride permeability of concretes with ground fly ash and slag. *Journal of Materials in Civil Engineering*, 21 (9), 494-501.
- [19] Barnett, S.J., Soutsos, M.N., Millard, S.G. and Bungey, J.H., 2006. Strength development of mortars containing ground granulated blast-furnace slag: Effect of curing temperature and determination of apparent activation energies. *Cement and Concrete Research*, 36 (3), 434-440.
- [20] Pack, S.W., Jung, M.S., Song, H.W., Kim, S.H. and Ann, K.Y., 2010. Prediction of time dependent chloride transport in concrete structures exposed to a marine environment. *Cement and Concrete Research*, 40 (2), 302-312.

- [21] Lounis, Z., 2003. Probabilistic modelling of chloride contamination and corrosion of concrete bridge structures. *In: Ayyub, B. and Attoh-Okine, N. eds. Proceedings of the fourth international symposium on uncertainty modeling and analysis (ISUMA '03)*, Maryland, USA.
- [22] Thoft-Christensen, P., Jensen, F.M., Middleton, C.R. and Blackmore, A., 1997. Assessment of the reliability of concrete slab bridges. *In: Frangopol, D.M., Corotis, R.B. and Rackwitz, R. eds. Reliability and optimization of structural systems*, London: Elsevier, 321-328.
- [23] Angst, U., Elsener, B., Larsen, C.K. and Vennesland, O., 2009. Critical chloride content in reinforced concrete – a review. *Cement and Concrete Research*, 39 (12), 1122–1138.
- [24] Schiessl, P. and Breit, W., 1996. Local repair measures at concrete structures damaged by reinforcement corrosion — aspects of durability. *In: Proceedings of the 4th international symposium on corrosion of reinforcement in concrete construction*, Cambridge, 525–534.
- [25] Gouda, V.K. and Halaka, W.Y., 1970. Corrosion and corrosion inhibition of reinforcing steel, II. Embedded in concrete. *British Corrosion Journal*, 5, 204–208.
- [26] Oh, B.H., Jang S.Y. and Shin, Y.S., 2003. Experimental investigation of the threshold chloride concentration for corrosion initiation in reinforced concrete structures. *Magazine of Concrete Research*, 55 (2), 117–124.
- [27] Val, D.V. and Stewart, M.G., 2003. Life-cycle cost analysis of reinforced concrete structures in marine environments. *Structural Safety*, 25(4), 343-362.
- [28] Melchers, R.E., 1999. *Structural reliability analysis and prediction*, 2nd edition, John Wiley & Sons Ltd., England.
- [29] Richardson, M.G., 1998. *Carbonation of reinforced concrete: Its causes and management*. Dublin: Citis.
- [30] Papadakis, V.G., Vayenas, C.G. and Fardis, M.N., 1991. Fundamental modeling and experimental investigation of concrete carbonation. *ACI Materials Journal*, 88 (4), 363-373.
- [31] Papadakis, V.G. and Tsimas, S., 2002. Supplementary cementing materials in concrete Part I: efficiency and design. *Cement and Concrete Research*, 32 (10), 1525-1532.
- [32] Sudret, B., Defaux, G. and Pendola, M., 2002. Time-variant finite element reliability analysis – application to the durability of cooling towers. *Structural Safety*, 27 (2), 93-112.
- [33] Stewart, M.G., Wang, X. and Nguyen, M., 2011. Climate change impact and risks of concrete infrastructure deterioration. *Engineering Structures*, 33 (4), 1326-1337.
- [34] Stipanovic Oslakovic, I., Bjegovic, D. and Mikulic, D., 2010. Evaluation of service life design models on concrete structures exposed to marine environment. *Materials and Structures*, 43 (10), 1397-1412.
- [35] Bastidas-Arteaga, E., Chateauneuf, A., Sánchez-Silva, M., Bressolette, Ph. and

Schoefs, F., 2011. A comprehensive probabilistic model of chloride ingress in unsaturated concrete. *Engineering Structures*, 33 (3), 720-730.

[36] Kwon, S.J., Na, U.J., Park, S.S. and Jung, S.H., 2009. Service life prediction of concrete wharves with early-aged crack: Probabilistic approach for chloride diffusion. *Structural Safety*, 31 (1), 75-83.

[37] Melchers, R.E., Li, C.Q., and Lawanwisut, W., 2008. Probabilistic modelling of structural deterioration of reinforced concrete beams under saline environment corrosion. *Structural Safety*, 30 (5), 447-460.

[38] Song, H.W., Park, S.W. and Ann, K.Y., 2009. Probabilistic assessment to predict the time to corrosion of steel in reinforced concrete tunnel box exposed to sea water. *Construction and Building Materials*, 23 (10), 3270-3278.

[39] Ferreira, R. M., 2008. Improving durability performance of reinforced concrete structures with probabilistic analysis. *International Journal of Concrete Structures and Materials*, 2 (2) 137-143.

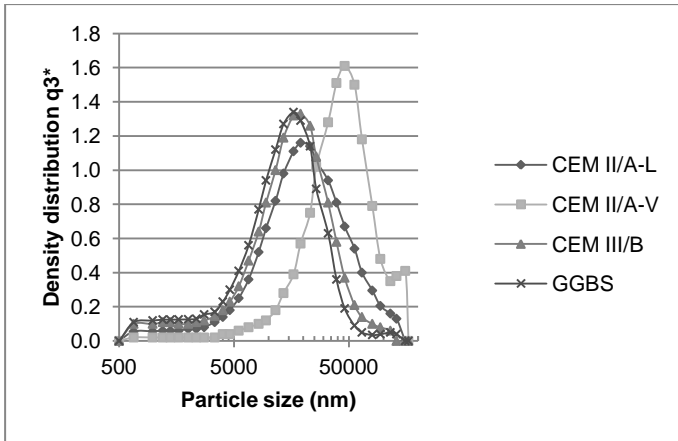


Fig. 1. Particle size analysis of cementitious binders used

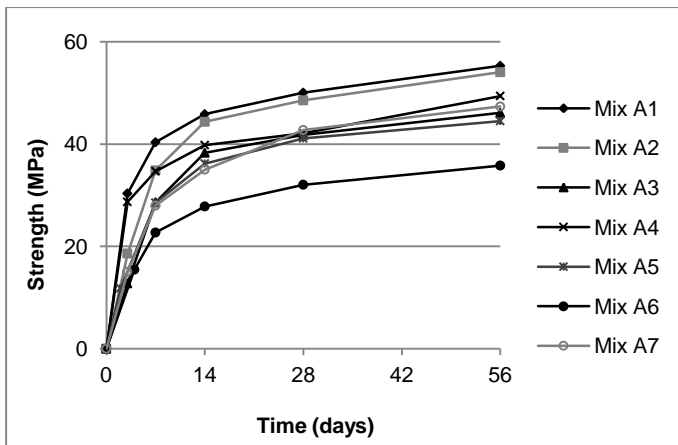


Fig. 2. Compressive strengths for binder contents 320 kg/m^3 , w/b ratio 0.55

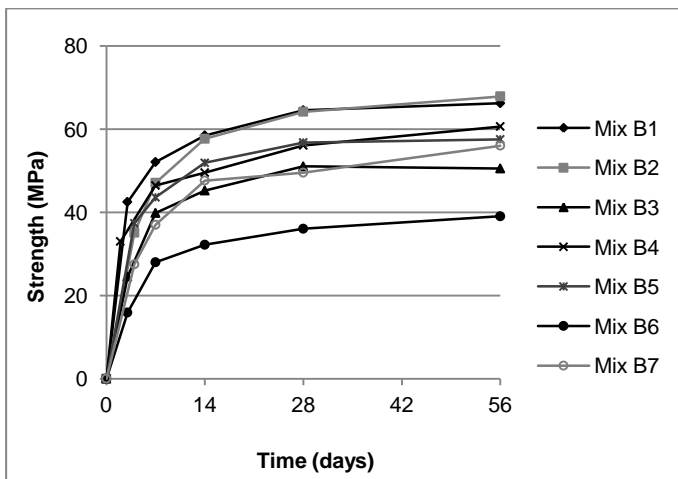


Fig. 3. Compressive strengths for binder contents 400 kg/m^3 , w/b ratio 0.45

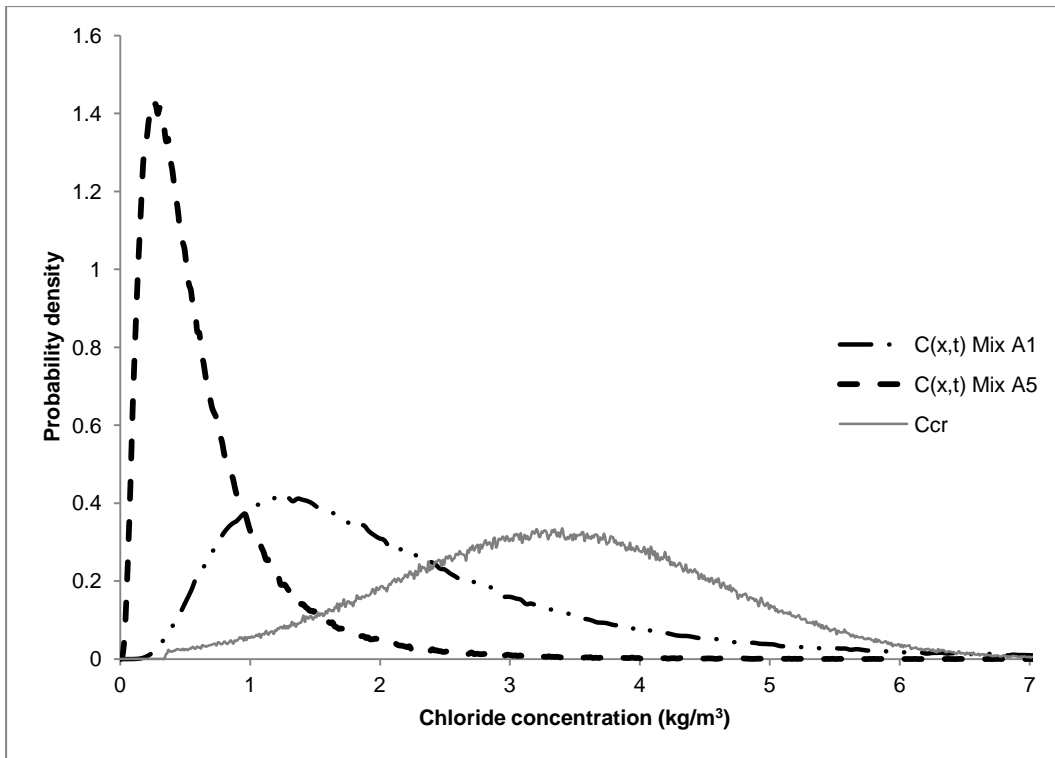


Fig. 4. Probability distribution for initiation of chloride induced corrosion for 2 binder combinations after 50 years

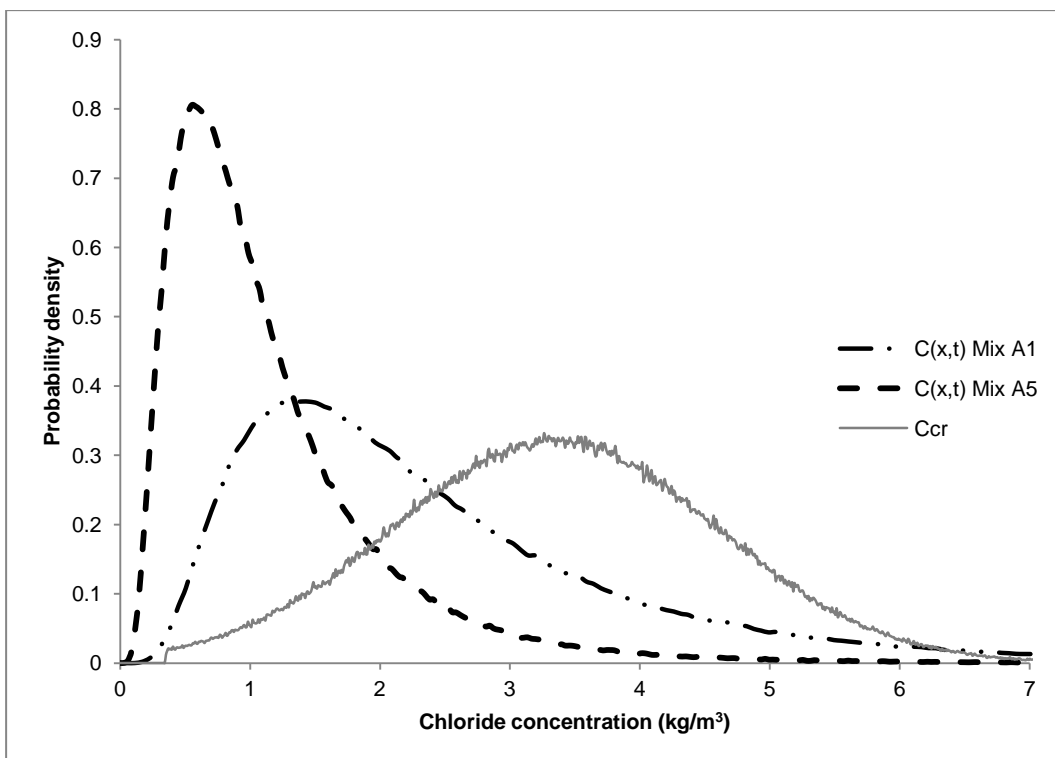


Fig. 5. Probability distribution for initiation of chloride induced corrosion for 2 binder combinations after 100 years

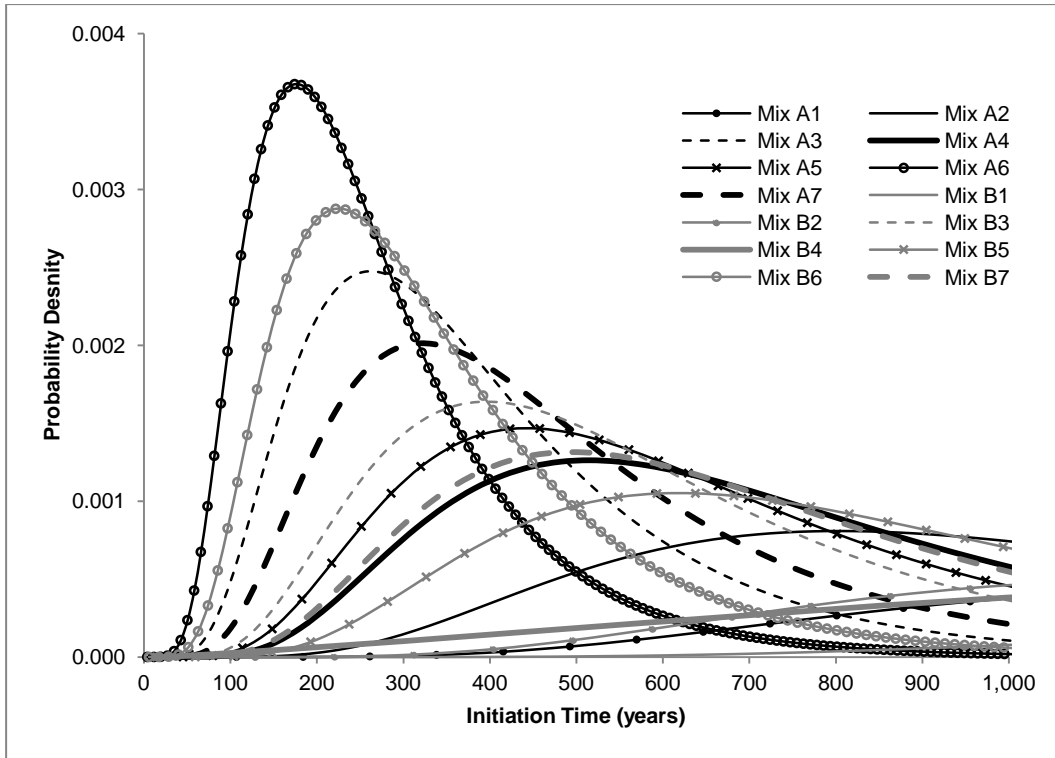


Fig. 6. Probability distribution for initiation of carbonation induced corrosion for various cementitious binders

Table 1 Some of the cement types permitted by EN 197

Type	Description	Clinker	Blast furnace slag	Siliceous fly ash	Limestone	Minor additional constituents
CEM I	CEM I	95-100	-	-	-	0-5
CEM II	CEM II/A-S	80-94	6-20	-	-	0-5
	CEM II/B-S	65-79	21-35	-	-	0-5
	CEM II/B-V	80-94	-	6-20	-	0-5
	CEM II/A-V	65-79	-	21-35	-	0-5
	CEM II/A-L	80-94	-	-	6-20	0-5
	CEM II/B-L	65-79	-	-	21-35	0-5
	CEM III	CEM III/A	35-64	36-65	-	-
CEM III/B		20-34	66-80	-	-	0-5
CEM III/C		5-19	81-95	-	-	0-5

Table 2 Basic mix designs used for testing

	Mix Type A	Mix Type B
Binder (kg/m ³)	320	400
C20 aggregate (kg/m ³)	800	770
C10 aggregate (kg/m ³)	400	385
Fine aggregate (kg/m ³)	700	665
Free water (kg/m ³)	176	180

Table 3 Chemical composition of binders used

Chemical Composition (% mass)	Binder Type			
	CEM II/A-L	CEM II/A-V	CEM III/B	GGBS
SiO ₂	19.8	21.0	31.4	35.1
Al ₂ O ₃	4.8	6.2	10.0	12.4
Fe ₂ O ₃	3.1	2.7	0.9	0.6
CaO	62.8	57.2	46.5	40.6
MgO	1.9	2.1	5.5	8.6
Mn ₃ O ₄	0.2	0.1	0.2	0.4
Na ₂ O	0.2	0.2	0.3	0.3
K ₂ O	0.6	0.7	0.6	0.4

Table 4 Binder combinations chosen for testing

Mix No	Cement Type	GGBS Level (%)	Binder Content	Water/Binder Ratio
A1	CEM II/A-L	0	320 kg/m ³	0.55
A2		50		
A3		70		
A4	CEM II/A-V	0		
A5		50		
A6		70		
A7	CEM III/B	0		
B1	CEM II/A-L	0	400 kg/m ³	0.45
B2		50		
B3		70		
B4	CEM II/A-V	0		
B5		50		
B6		70		
B7	CEM III/B	0		

Table 5 Resistance of various binder combinations to chloride ingress and carbonation

Mix No	Cement Type	GGBS Level (%)	D _R (x10 ⁻¹² m ² /s)	Carbonation Depth (mm)		
				7 days	28 days	56 days
A1	CEM II/A-L	0	14.2	4.6	5.2	7.1
A2		50	1.3	3.7	7.5	9.8
A3		70	0.77	7.3	8.8	19.9
A4	CEM II/A-V	0	9.14	5.5	8.7	12.4
A5		50	1.22	6.1	9.4	13.3
A6		70	1.73	7.9	14.6	21.9
A7	CEM III/B	0	0.81	7.4	9.2	16.8
B1	CEM II/A-L	0	7.01	3.2	4.5	5.3
B2		50	0.81	3.4	3.6	9.3
B3		70	1	5.6	11	13.6
B4	CEM II/A-V	0	4.15	4.4	7.6	7.9
B5		50	1.95	6	8.6	10.5
B6		70	0.85	10.1	13.7	17.7
B7	CEM III/B	0	1.07	6.7	10.4	11.2

Table 6 Time dependent diffusion coefficient at 50 years and 100 years

Mix No	Cement Type	GGBS Level (%)	D_R ($\times 10^{-12} \text{ m}^2/\text{s}$)	D_m ($\times 10^{-12} \text{ m}^2/\text{s}$)	
				50 years	100 years
A1	CEM II/A-L	0	14.20	11.05	10.85
A2		50	1.30	0.51	0.47
A3		70	0.77	0.30	0.28
A4	CEM II/A-V	0	9.14	7.11	6.98
A5		50	1.22	0.48	0.44
A6		70	1.73	0.68	0.62
A7	CEM III/B	0	0.81	0.32	0.29
B1	CEM II/A-L	0	7.01	5.46	5.36
B2		50	0.81	0.32	0.29
B3		70	1.00	0.39	0.36
B4	CEM II/A-V	0	4.15	3.23	3.17
B5		50	1.95	0.76	0.70
B6		70	0.85	0.33	0.31
B7	CEM III/B	0	1.07	0.42	0.39

Table 7 Parameters used for deterioration models

Variable	Mean	COV	Distribution
Cover [27]	50 mm	Standard deviation=10 mm	Normal
Critical chloride concentration [27]	3.35 kg/m^3	0.375	Normal; truncated at 0.35 kg/m^3
Surface chloride concentration [27]	2.95 kg/m^3	0.7	Lognormal
Effective chloride diffusion coefficient, based on [27]	Varies, based on data from Table 6	0.2	Normal
CO ₂ concentration, based on [32]	0.05%	0.25	Lognormal
Effective CO ₂ diffusion coefficient, based on [27]	Varies, based on data from Table 6	0.2	Normal

Table 8 Probability of corrosion after service life of 50 years and 100 years

Mix No	Cement Type	GGBS Level (%)	Probability of Chloride Induced Corrosion		Probability of Carbonation Induced Corrosion	
			50 years	100 years	50 years	100 years
A1	CEM II/A-L	0	0.242	0.280	6.15E-12	2.10E-08
A2		50	0.017	0.050	5.06E-09	4.65E-06
A3		70	0.005	0.022	1.40E-04	9.57E-03
A4	CEM II/A-V	0	0.223	0.256	4.98E-07	1.56E-04
A5		50	0.028	0.059	1.98E-06	4.47E-04
A6		70	0.035	0.070	1.92E-03	5.51E-02
A7	CEM III/B	0	0.008	0.029	2.93E-05	3.20E-03
B1	CEM II/A-L	0	0.205	0.234	5.64E-15	5.98E-11
B2		50	0.005	0.021	2.29E-11	6.01E-08
B3		70	0.011	0.052	5.30E-06	9.27E-04
B4	CEM II/A-V	0	0.136	0.177	5.06E-10	7.48E-07
B5		50	0.050	0.079	7.91E-08	3.95E-05
B6		70	0.008	0.033	4.02E-04	1.97E-02
B7	CEM III/B	0	0.013	0.038	7.35E-07	2.09E-04